Lab 1 Report

Kalie Knecht, Ian Kolaja, and Trevor Arino

November 6, 2022

Introduction

When a detector is operated such that the amount of signal generated is proportional to the amount of energy deposited, it is possible to know the energy of the incident particle. Detectors offering energy detection has allowed the possibility for gamma-ray spectroscopy [4], which can be used in a variety of applications, including source identification and radiation imaging. Semiconductor detectors are one type of detector which is sensitive to radiation energy. High Purity Germanium (HPGe) Detectors are one type of semiconductor detectors which are commonly used for gamma-ray spectroscopy. HPGe detectors have excellent energy resolution, but are not largely portable because they require cooling, usually through liquid Nitrogen (LN). The excellent energy resolution makes HPGe detectors preferable for gamma-ray spectroscopy, particularly when there are many peaks that are close together, which might not be distinguishable in a detector with low energy resolution.

In this experiment, a pulse processing chain is developed for an HPGe detector. Raw waveforms from the detector are shaped with a trapezoidal filter and binned into a spectrum based on trapezoid height. An energy and energy resolution calibration routine is developed for this spectrum using check sources, and the resulting spectrum is analyzed to determine detector characteristics.

Methods

0.1 Detector Acquisition System

0.1.1 Detector Setup

In this experiment, we used a LN-cooled co-axial HPGe detector biased at 3200 V. The HPGe detector is connected to a pre-amplifer which is housed within the detector cryostat to reduce noise. The pre-amplifer output cable is connected to a Struck Innovation Systems (SIS) 16 Channel VME Digitizer card, which sends raw digitized pulse waveforms to a computer via an ethernet cable.

The *Ethernet Data Aquisition Code for SIS3316 250MHz Digitizers data acquisition software* package from the BeARING github [1] is used to aquire data from the detector with the digitizer. The data acquisition parameters are customizable through a JSON configuration file. Example JSON configuration files were provided in the software repository, which were modified to better serve our purposes for this laboratory. The main changes made to the configuration were:

- **Pre-Trigger Delay**: set at max setting allowed by SIS software to collect sufficient baseline. Set at 1000.
- **Trigger Threshold Value**: chosen in an iterative method such that low energy noise was reduced, but low energy gamma peaks were still visible in the resulting spectra. Set at 5000.

Isotope	Activity 10/28/22 [μCi]	Energy [kev]	Intensity [%]
Ba-133	5.26	383.9	8.94
Cs-137	8.21	661.7	85.1
Co-60	2.46	1173.2	99.85
Co-60	2.46	1332.5	99.98

Table 1: Check sources used in the laboratory with their activity and associated gamma-ray energies and intensities from [2]

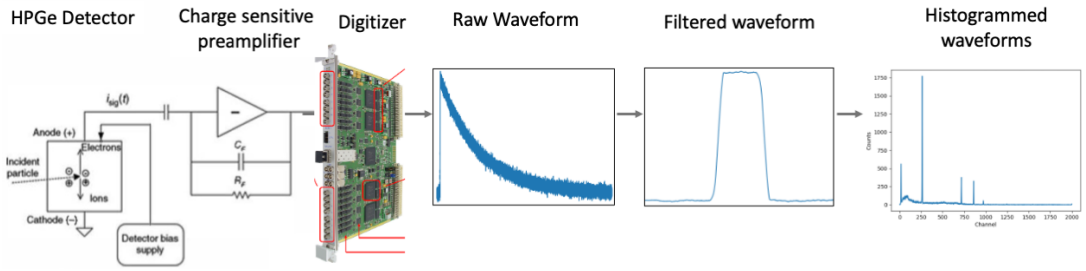

Figure 1: Pulse processing chain of HPGe detector setup, modified from [4].

- **Sample Length**: determined by viewing pre-amplifier pulses on an oscilloscope. The sample length is selected such that the sharp rise and long decay are captured in the digitized waveform. Set at 50,000.

The complete configuration file used for data acquisition may be found in App. A.

A series of check sources were used to calibrate the detector. Co-60, Ba-133, and Cs-137 check sources were used placed at a 25 cm source-to-detector distance on axis with the detector. The check sources were each measured separately for 10 minutes to reduce pile-up and high count rate effects in our calibration procedure. The relevant source peak energies, activities, and associated isotopes are summarized in Table 1.

0.1.2 Shaping Filter

The output from the SIS digitizer consists of raw pre-amplifier pulses, which must be filtered before performing spectroscopy. A common choice for HPGe detectors is a a trapezoidal shaping filter, which performs baseline correction, pole-zero correction, and pulse shaping resulting in a flat top pulse. The pulse height can then be extracted to perform spectroscopy.

For this experiment, we used the trapezoidal shaping filter described by Cooper [3], implemented in python by Jaewon Lee.

The optimal tau, peaking time, and gap time were determined experimentally. The tau value was selected by fitting an exponential to a random sample of the raw pulse waveforms. The peaking time and gap time were determined by iterating through different values and selecting those which resulted in the lowest energy resolution.

The pulse processing chain used to collect and analyze data for this experiment is summarized in Fig. 1.

0.2 Detector calibration

0.2.1 Energy Calibration

The heights of the trapezoid pulses from the shaping filter are proportional to energy deposited in the detector. The maximum height of the trapezoids are histogrammed into 2000 bins, with the minimum range imposed by the DAQ trigger threshold and maximum range cut to the

99.5% quantile of data. This results in a dynamic range of around 350 keV - 2.6 MeV. The histogram bins are converted from trapezoid heights to channel numbers of 0 - 2000, correlated to the center of each histogram bin.

In a HPGe detector, we expect to see a linear relationship between pulse height (channel number) and energy deposited in the detector [4]. Therefore, the energy calibration is determined by performing a linear regression on the peak channel numbers and known gamma-ray energies. The peak channel numbers are determined by using a peak fitting algorithm to roughly approximate the peak centroid, which is then refined with a Gaussian fit. The source energies from Table 1 are then used to correlate the channel number of each peak in the histogram with energy. We expect this calibration to hold true for future experiments with this detector, so it may be saved for use in future experiments.

0.2.2 Energy Resolution Calibration

The sigma parameter obtained from the gaussian curve fit is scaled by the slope of the energy calibration to find the sigma of each peak in units of energy. The Full Width Half Max (FWHM) is then calculated through:

$$FWHM = 2.355\sigma$$

The energy resolution is calculated as:

$$\text{Energy Resolution} = \frac{FWHM}{E} \tag{1}$$

0.2.3 Fano Factor

The Fano factor (F) quantifies the departure of observed statistical fluctuations in the number of charge carriers from pure Poisson statistics, or:

$$F = \frac{\text{observed variance}}{\text{Poisson predicted variance}}$$

For HPGe detectors, the Fano factor is expected to be less than 1, meaning that the observed variance in HPGe detectors is less than what is predicted by Poisson statistics. The Fano factor can be found with the fitted energy FWHM of gamma-ray peaks, through the relation:

$$FWHM = \sqrt{\Delta E_{stat}^2 - \Delta E_{noise}^2}$$

if ΔE_{noise} can be measured experimentally. ΔE_{stat} can be found through:

$$\Delta E_{stat} = 2.355\sqrt{FE_\gamma W}$$

where:

- E_γ is the energy of the gamma-ray, and
- W is the energy required to generate an electron-hole pair in detector medium (2.96 eV in Ge).

Rearranging these two equations gives:

$$F = \frac{FWHM^2 - \Delta E_{noise}^2}{2.355^2 E_\gamma W} \tag{2}$$

For this experiment, we experimentally determined the noise contribution ΔE_{noise} to to find the Fano factor of our detector.

We measure the noise contribution by connecting a pulse generator to the test input of the pre-amplifier. We then generate a pulse that is 7 ms wide, with a frequency of 30 Hz. The height of the pulse was set to the lowest value possible at 300 mV. We then collected data over a period of 10 minutes and analyzed the pulses through our pulse processing chain, ultimately finding the FWHM of the pulser peak in keV, which is ΔE_{noise} for our detector setup.

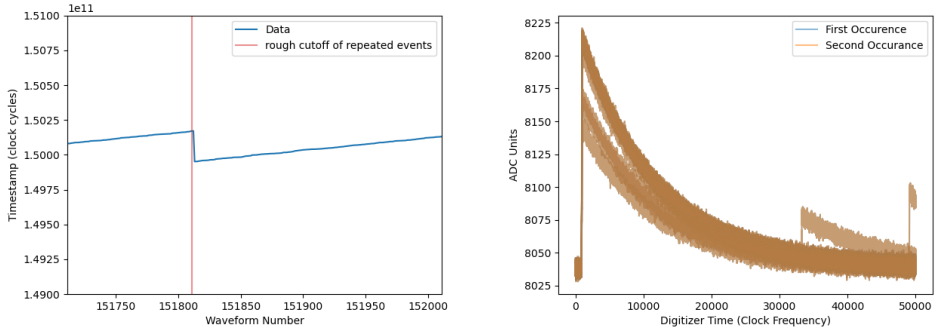

Figure 2: Left: Data acquisition echo, resulting in repeated events at the end of the savefile. Events with duplicate timestamps are removed from the data before any data analysis. Right: Verification that the events with duplicated timestamps are the same waveforms.

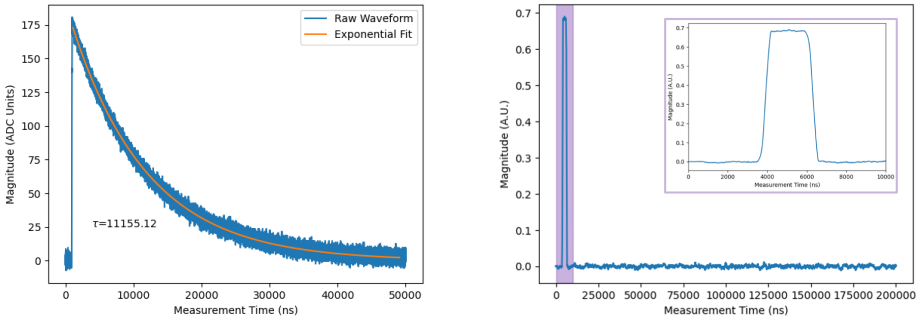

Figure 3: Left: Example raw waveform from Struck digitizer, Right: waveform after applying trapezoidal filter, with inset zoomed to the purple region of the plot

Results

0.3 Pulse Processing

There is an 'echo' present at the end of each data acquisition (shown in Fig. 2, left), so the data must first be cleaned to remove repeated waveforms. Fig. 2 right verifies that these duplicate events show the same waveform data. Following data cleaning, the 10-minute measurements obtained 152,057 Cs-137 waveforms, 138,945 Co-60 waveforms, and 8,822 Ba waveforms.

An example raw waveform pulse is shown in Fig. 3, left. The exponential fit and the time constant (in units of clock frequency) for this pulse are also displayed on the figure. The average time constant from a subset of the waveforms is used for the trapezoidal filter. The experimentally determined filter parameters used in our pulse processing chain are:

- $\tau = 4.387 \times 10^5$ s
- peaking time $= 4 \times 10^{-7}$ s
- gap time $= 2 \times 10^{-6}$ s

Applying the shaping filter with these parameters to this raw waveform results in a trapezoidal pulse shown in Fig. 3, right.

0.4 Detector Calibration

Figure 4, left displays the concept that trapezoidal pulse heights are proportional to the energy deposited in the detector. The raw histogram of binned trapezoid heights is shown in Figure 4,

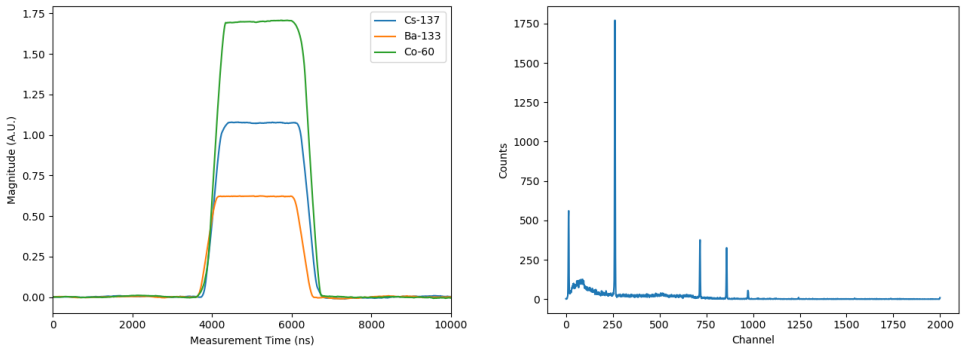

Figure 4: Left: Trapezoid heights of example pulses from data collections of individual sources, Right: Histogrammed trapezoid heights

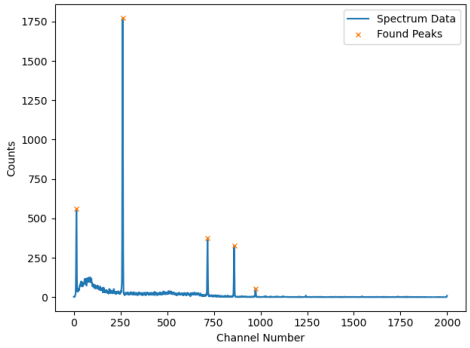

Figure 5: Peak finding algorithm results. This is an initial guess of the peak location, which is then refined through Gaussian fitting with an energy window half-width of 10 keV.

right. In addition to the four gamma-ray peaks we expected to see from our check sources, we see a background peak which is likely from K-40. We did not subtract background from our spectrum, and instead opted to use visible background peaks as additional points for our energy calibration.

0.4.1 Energy Calibration

The approximate peak channel numbers selected by the peak fitting algorithm are shown in Fig. 5. The energies of selected gamma-ray peaks in ascending order are the 383.8 keV peak of Ba-133, 662 keV peak of Cs-137, 1173 and 1332 keV peaks of Co-60, and the 1461 keV peak associated with K-40 (background). The linear fit on the channel numbers associated with these energies is shown in Fig. 6 left, and the resulting energy calibrated spectrum is shown in Fig. 6 right.

0.4.2 Energy Resolution Calibration

The gaussian curve fitting and resulting FWHM for each of the four source peaks is shown in Fig 7, left. The FWHMs compared with peak energy are shown in Fig 7, middle. Fig 7, right shows the energy resolution of each of the source peaks, calculated with Equation 1. As expected, the energy resolution decreases with source energy.

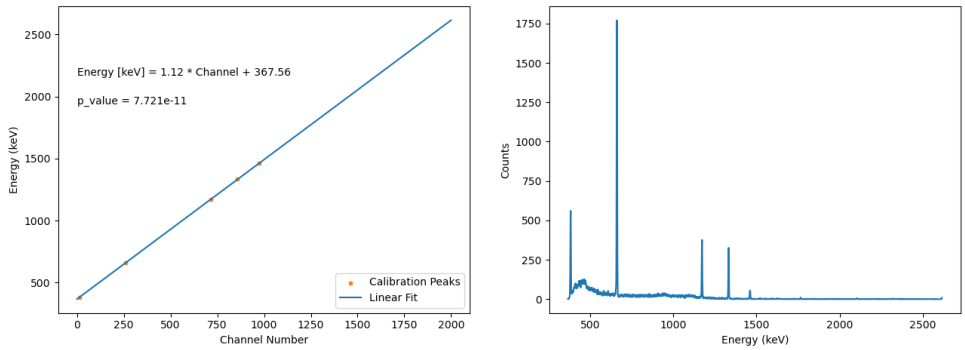

Figure 6: Left: Energy vs channel linear fit, with energy calibration equation, Right: Energy calibrated spectrum

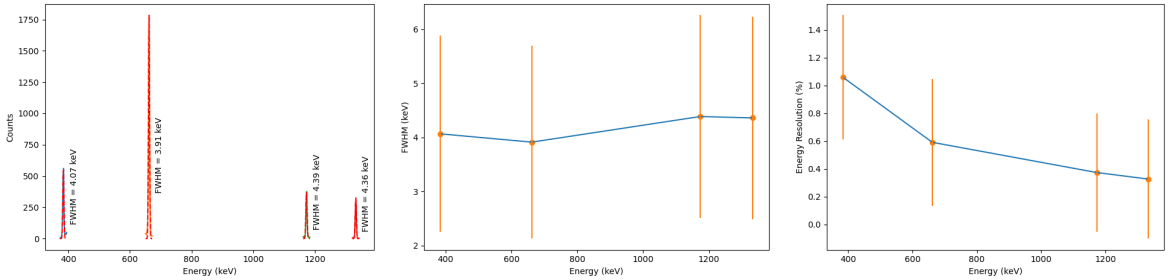

Figure 7: Left: Gaussian curve fitting on the source peaks and associated FWHM values, Middle: FWHMs of source peaks plotted vs peak energy, Right: Energy resolution determined for each of the source peaks.

0.4.3 Fano Factor

The experimentally determined ΔE_{noise} from the FWHM of our pulser peak is 2.72 keV. With this value known, it was possible to calculate the Fano factor with Equation 2. We determined the value of the Fano factor for each of our source peaks and found the average value to generate a Fano factor that is representative of our detector across its dynamic range. The Fano factor determined for each of the source peaks is shown in Fig. 8. The average was determined to be 0.68.

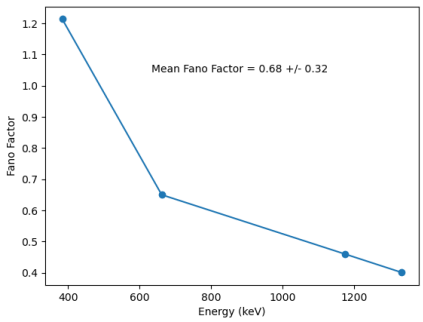

Figure 8: Fano Factor

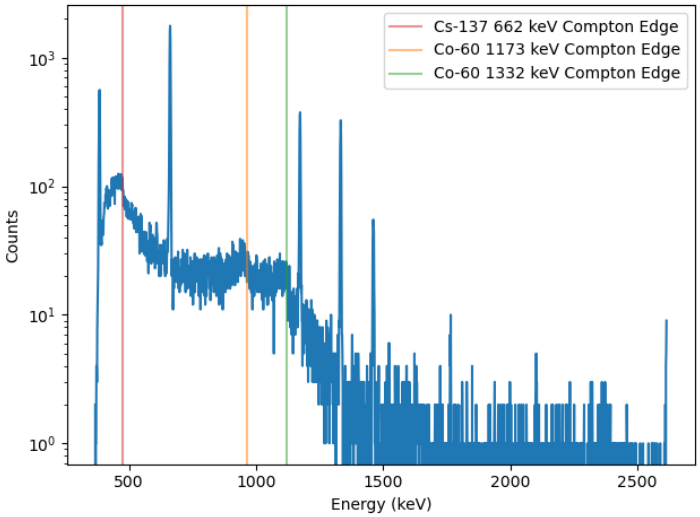

Figure 9: Energy spectrum on semilog scale with expected Compton edge energies shown.

Discussion

0.5 Spectral feature discussion

When plotted on a semilog scale, more features of the gamma-ray spectrum are easily visible. The energy spectrum of our data on a semilog scale can be found in Fig. 9. In Ge (Z=32) we expect Compton scattering to become the dominant interaction mechanism at just below 200 keV. This means for a photopeak to occur, these high energy photons must undergo Compton scattering and then a photoelectric interaction for their full energy to be deposited. Due to the small size of the HPGe crystal, a photon can undergo Compton scattering and then leave the detector, therefore a Compton continuum can be seen. The high energy end of the Compton continuum is called the Compton edge, which can be calculated through the Compton formula,

$$E_c = \left(1 - \frac{1}{1 + \frac{E_0}{m_e c^2}(1 - cos\theta)}\right) E_0$$

where:

- E_c is the Compton edge energy,
- $m_e c^2$ is the rest mass of an electron (511 keV),
- θ is the scattering angle of the gamma-ray (=180^o for Compton Edge), and
- E_0 is the incident gamma-ray energy.

The Compton edges energies for our gamma-ray peaks are shown in Table 2. Due to the high trigger threshold in our DAQ settings, the dynamic range of our detector begins at around 350 keV. While it might be possible to see a Compton edge for the 384 keV Ba-133 peak, our dynamic range is such that it is only possible to see the photopeak of this gamma-ray. However, we do expect to see a Compton edge for the Cs-137 and Co-60 peaks. Fig. 9 shows these expected Compton edge energies on the energy spectrum, and we can see the Compton edges visible in the expected locations.

Due to small size of crystal, it is also possible to see escape peaks from the Co-60 lines, since they exceed the threshold energy of pair production (1.022 MeV). Escape peaks occur when the photons resulting from positron annihilation escape the detector. However, we do not see any notable escape peaks in our spectrum.

Peak Energy (keV)	Compton Edge (keV)	Possible to see
384	230.5	No
662	477.7	Yes
1173	963.2	Yes
1332	1117.6	Yes

Table 2: Compton Edge energies

0.6 Detector Acquisition System Discussion

The Data Acquisition software required quite the learning curve and many iterations to produce quality results. Despite the effort in finding a configuration that worked best, there are still issues present in the software that should be addressed, such as the 'echo' of repeated events at the end of the data acquisition.

The Trigger Threshold Value is set too high to see lower energy peaks of Ba-133. It would be better to have lower energy peak to extend the lower end of our detector's dynamic range and to have additional low energy points for our energy and energy resolution calibration. We could reduce this threshold further, but must keep in mind that lowering it might also yield low energy noise.

We could also improve our filtering techniques. Currently we run into computational memory issues when filtering and storing all of our pulses, so we must downsample our data. We could improve efficiency in the code or use caching to improve our current filter, or we could investigate using other filters to achieve our goals.

0.7 Calibration discussion

The energy calibration determined in the experiment was linear as we expected. We could improve our confidence in our calibration by using more gamma-ray energies when calibrating our detector by using more check sources or taking longer counts of our background. We did not have a lot of counts in our background peaks because we did not have a dedicated background measurement, and instead just used the small peaks that appeared over the 30 minutes of measurement time. There were two complete background peaks visible in our spectrum, but only the 1461 KeV K-40 peak was large enough to be identified by our peak finding algorithm. The second smaller background peak is around 1764 keV, which is associated with Bi-214. There is an additional small background peak from Tl-208 found near 2614 keV, however only the left tail of the peak is visible due to the maximum range imposed in our histogramming method. For future experiments, we should increase this histogram threshold or remove it entirely to make this peak more visible.

Because there are not a lot of counts in the K-40 peak, this peak was removed from our energy resolution fitting, which is not ideal. To get better use of this background peak to include in our energy resolution calibration, we could collect background data over a longer period of time.

The code developed for our calibration routine is not currently handling pileup correctly. When histogramming our counts, we simply take the maximum value of the trapezoid filtered pulses, effectively counting a piled-up pulse as one single pulse. In future experiments, we will be analyzing high count rate data, so we will want to develop methods to properly obtain the pulse height of each of the piled up pulses.

Our averaged Fano factor was determined to be 0.68, which is larger than the value of 0.13 which is typical of HPGe detectors [4]. The larger value means that we are closer to what we would expect from Poisson statistics, and have a worse resolution than what is expected in HPGe detectors. We could perhaps improve our energy resolution by improving our trapezoidal filtering or determining issues, if any, that might be arising from our data acquisition software.

However, given the age and brutal treatment of this detector in the teaching laboratory, a Fano factor of 0.68 might be approaching the best performance we can achieve.

During this experiment, there was quite the scare that someone (definitely not me) might have damaged the pre-amplifer of the HPGe detector by applying a voltage to the detector while the pre-amplifer was not plugged into a power source. This might warrant further analysis, but whoever might have damaged the pre-amp (still not me) is probably sleeping better at night given the 2.72 keV ΔE_{noise} determined in this experiment. This value is not fantastic, but it is about the same that it was was one year ago in Fall 2021 NE 104 lab reports. The electronic noise contribution could be further reduced by changing out the cables which have probably been dropped on the floor. Should the pre-amp be damaged, replacing it would decrease the noise contribution further, but that would really suck for the person that broke it (NOT ME) because they would never hear the end of it from Kai.

0.8 Conclusions

In this laboratory, we developed software that can quickly filter waveforms and find an energy and energy resolution calibration. We found that the energy calibration was linear as expected. We also found that our energy resolution decreased with peak energy, but our energy resolution is not quite as good as what is typically cited for HPGe detectors. There is room for improvement in the methods developed in this experiment; however, the initial methods developed were a great learning exercise for how pulse processing generally works, as well as how to troubleshoot stubborn data acquisition software. The methods developed for this experiment will be further improved for future experiments which will involve more complicated measurement scenarios, such as high count rate measurements and Compton scattering analysis.

References

[1] BeARING. *Ethernet Data Aquisition Code for SIS3316 250MHz Digitizers*. `https://github.com/bearing/python3316/tree/raw_waveform_fix_later`. 2021.

[2] National Nuclear Data Center. *NuDat 2.8*. `https://www.nndc.bnl.gov/nudat3/nudat2.jsp`. 1996.

[3] R Cooper. "Digital Gamma-Ray Spectroscopy: Trapezoidal Filtering". en. In: (2013), p. 4.

[4] Glenn F. Knoll. *Radiation detection and measurement*. en. 4th ed. OCLC: ocn612350364. Hoboken, N.J: John Wiley, 2010. ISBN: 978-0-470-13148-0.

Appendix

A

JSON Config File


```
{"Accumulators": {
        "Gate 1": {
            "Length": 50,
            "Start Index": 0
        },
        "Gate 2": {
            "Length": 50,
            "Start Index": 100
        },
        "Gate 3": {
            "Length": 0,
            "Start Index": 0
        },
        "Gate 4": {
            "Length": 0,
            "Start Index": 0
        },
        "Gate 5": {
            "Length": 0,
            "Start Index": 0
        },
        "Gate 6": {
            "Length": 0,
            "Start Index": 0
        },
        "Gate 7": {
            "Length": 0,
            "Start Index": 0
        },
        "Gate 8": {
            "Length": 0,
            "Start Index": 0
        }
    },
    "Address Threshold": 250000,
    "Analog/DAC Settings": {
        "50 Ohm Termination": true,
        "DAC Offset": 32768,
        "Input Range Voltage": 1
    },
    "Clock Settings": {
        "Clock Distribution": 0,
        "Clock Frequency": 250
    },
    "Energy Filter": {
        "Gap Time": null,
```

```
    "Peaking Time": null,
    "Tau Factor": null,
    "Tau Table": null
},
"Event Settings": {
    "External Gate": false,
    "External Trigger": false,
    "External Veto": 0,
    "Internal Gate 1": 0,
    "Internal Gate 2": 0,
    "Internal Trigger": true,
    "Invert Signal": false,
    "Sum Trigger Enable": false
},
"Hit Data": {
    "Accumulator Gates 1-6 Flag": true,
    "Accumulator Gates 7-8 Flag": false,
    "Energy MAW Flag": false,
    "MAW Test Buffer": false,
    "MAW Values Flag": false
},
"MAW Settings": {
    "MAW Test Buffer Delay": 0,
    "MAW Test Buffer Length": 0,
    "MAW Test Buffer Select": 0
},
"Module Info": {
    "Last 3 Serial Number Digits": 66,
    "Name": "Chris_CAMIS",
    "ip address": "192.168.1.10"
},
"Trigger/Save Settings": {
    "CFD Enable": 0,
    "Gap Time": 50,
    "High Energy Threshold": 10000,
    "Peaking Time": 50,
    "Pile Up": 0,
    "Pre-Trigger Delay": 1000,
    "Pre-Trigger P+G Bit": 0,
    "Re-Pile Up": null,
    "Sample Length": 50000,
    "Sample Start Index": 0,
    "Sum Trigger CFD Enable": 0,
    "Sum Trigger Gap Time": 0,
    "Sum Trigger High Energy Threshold": 0,
    "Sum Trigger Peaking Time": 0,
    "Sum Trigger Threshold Value": 0,
    "Trigger Gate Window": 100,
    "Trigger Threshold Value": 5000
}}
```